Nanomechanical Response of Bacterial Cells to Cationic Antimicrobial Peptides

Supplementary Information

Shun Lu, Grant Walters, Richard Parg and John R. Dutcher[*]

Department of Physics, University of Guelph, Guelph, Ontario, Canada N1G 2W1

[*] Corresponding author: John Dutcher, Department of Physics, University of Guelph, Guelph, Ontario, Canada N1G 2W1; Tel: 519-824-4120, ext. 53950; Fax: 519-836-9967; Email: dutcher@uoguelph.ca

SI1. AFM topography images and representative line scans of *P. aeruginosa* PAO1 Cells Before and After Exposure to Peptides

AFM topography images and representative line scans of *P. aeruginosa* PAO1 cells before and after exposure to PMB and PMBN are shown in Fig. S1. Histograms of cell heights measured before and after more than 1 h of exposure to PMBN are shown in Fig. S1(c).

SI2. AFM Creep Deformation Measurements Performed on *P. aeruginosa* PAO1 Cells at Large Forces

Before exposure to the cationic peptides, we are able to analyze the creep deformation curves using the Standard Solid Model since the deformation reaches a plateau value at long times. Under these conditions, the deformation of the cells is reversible, since the integrity of the bacterial cell envelope is intact. In a previous study,[37] we showed that complete recovery of the cell shape was obtained in AFM images following large deformations of *P. aeruginosa* PAO1 cells induced by large loading forces during AFM imaging. In Milli-Q water, the cell height is the same to within the uncertainty of the measurement before and after a creep measurement at 6.0 nN, as shown in the AFM line scans shown in Fig. S2(a). However, after a sufficient time of exposure to 50 µg/mL PMB and PMBN, the application of a large force causes a significant irreversible decrease in the cell height. For example, the application of $F_0 = 6.0$ nN for 6.0 s to cells exposed to PMB typically caused an irreversible decrease in cell height of 15 nm, as can be seen by comparing the line scans for the large cell centered at 2 µm in Fig. S2(b) (same cell as in Fig. S2(a)) measured before and after the creep deformation experiment. It can be seen in Fig. S2(b) that the line scans also include a second smaller cell centered at ~3.5 µm (not present in Fig. S2(a)). It is interesting to note that there is no measurable decrease in cell height between the two line scans for the smaller cell on which the creep deformation experiment was not performed. In Fig. S2(c), it can be seen that the decrease in cell height after the creep deformation experiment is even more significant at larger forces: the application of $F_0 = 20.0$ nN for 6.0 s to cells exposed to PMB typically caused an irreversible decrease in the cell height of 45 nm. This decrease in cell height is likely due to molecules being forced out of the cell by the

applied force F_0. Because of this, it is necessary to apply small forces ($F_0 < 4$ nN) to measure the time-resolved mechanical response of bacterial cells to cationic peptides.

SI3. Analysis of the AFM Creep Deformation Experiment in Terms of the Theory of Poroelasticity

Poroelasticity accounts for the flow of solvent molecules in addition to the mechanical deformation of the underlying network structure. It has been applied successfully to mechanical measurements of hydrogels[51] and, more recently, to eukaryotic cells.[52] In these studies, solvent flow occurs over sufficiently large length scales that it is observed within the time scale of the experiment. However, for the present measurements involving nanoscale deformation of individual bacterial cells, a constant force, which can be varied between 4.0-10.0 nN, is applied by the AFM cantilever to the cell during a loading time $t_L \sim 50$ ms, resulting in a cellular indentation δ of up to 100 nm, The timescale for the movement of water in hydrogels due to deformation by a probe of radius R is characterized by the characteristic poroelastic time $t_D \sim \delta R/D_p$, where D_p is the poroelastic diffusion coefficient, which has been estimated as 1-100 μm^2/s for cells.[52] Given that the radius of the AFM tip in the present study is $R = 300$ nm, the characteristic poroelastic time for the bacterial cells is $t_D \sim 0.3$-30 ms. Thus, the deformation is sufficiently small that solvent flow occurs much faster (typically within milliseconds) than the observed characteristic response times in the creep deformation measurements (of the order of a second).

In contrast to the exponential relaxation of linear viscoelastic materials, which have the form, $F(t) \sim F_0 \exp(-t/\tau)$, and power law relaxations, which have the form $F(t) \sim F_0 (t/t_0)^{\beta}$, the characteristic relaxation time of force-relaxation curves for poroelastic materials depends on the length scale of the measurement. This means that the normalization of relaxation curves of poroelastic materials to create a "master curve" requires scaling of both force (F/F_0) and time (t/δ). However, as shown in Fig. S3, we find that the force-relaxation curves collected on *P. aeruginosa* PAO1 bacterial cells with different applied forces F_0 can be normalized to a master curve by just scaling the force and not scaling the time. As a result, the force-relaxation behaviour can be characterized by a simple single exponential relaxation for the bacterial cells, and this further justifies

the validity of the viscoelastic models that we have used to analyze the creep deformation curves in the present study.

After exposure to PMB and PMBN, which compromises the mechanical integrity of the bacterial cell envelope, there is likely flow of molecules out of the periplasm and/or interior of the cell, and it is possible that this behaviour could be understood in terms of the poroelastic properties of the compromised bacterial cell envelope. This will be the subject of further study.

SI4. Correlation of Delayed Elastic Parameters with Permeability Parameter After Exposure to PMB and PMBN

In Fig. S4, we show a plot of the best-fit values of the delayed elastic parameter k_2 versus the permeability parameter $1/\eta_1$ before and after exposure to PMB and PMBN. Before exposure, we observed values of $1/\eta_1$ centered narrowly about zero (see Figs. 3 and 4). After exposure to either PMB or PMBN, we observed a well-defined negative slope in the plots shown in Fig. S4, which corresponded to smaller values of k_2 and nonzero values of $1/\eta_1$. Similar correlations are observed between the delayed elastic parameter η_2 and the permeability parameter $1/\eta_1$.

SI5. AFM Creep Deformation Measurements Performed on *P. aeruginosa wapR* Mutant Cells

AFM creep deformation experiments were performed on *P. aeruginosa wapR* mutant cells. These bacterial cells have LPS molecules that have an intact outer core, but lack the hair-like O-antigen side chains.[S1] The resulting histograms of the best-fit viscoelastic parameters are shown in Fig. S5. If the delayed elastic response observed for wild type cells was due to the LPS O-antigen side chains, we would expect that the results measured for the *wapR* LPS mutant cells would yield a larger values of k_2. However, as shown in Fig. S5, we measured k_2 and η_2 values for the *wapR* LPS mutant cells that were significantly less (by roughly a factor of 2) than those values measured for the wild type cells (see Table I). There are a significant number of cells that have a small but nonzero permeability parameter $1/\eta_1$. This small amount of permeability is likely related to a reduced tolerance of the cells for Milli-Q water due to the lack of the O-

antigen side chains in the LPS molecules. This probably leads to some degree of dilution of the periplasm that results in reduced values of k_2 and η_2. There is a small negative correlation between the delayed elastic parameter k_2 and $1/\eta_1$ (see Fig. S5(e)).

SI6. AFM Creep Deformation Measurements Performed on *P. aeruginosa* PAO1 Cells at a Lower Concentration of PMB and PMBN

We performed AFM creep deformation experiments on *P. aeruginosa* PAO1 cells before and after exposure for 1 h to a lower PMB concentration of 5.0 μg/mL. The resulting histograms of the best-fit viscoelastic parameters are shown in Fig. S6. Following exposure to the low PMB concentration, most of the cells had small but nonzero values of $1/\eta_1$, showing that the cell envelope integrity was compromised, but to a lesser extent than for the larger PMB concentration (Fig. 3). Interestingly, a large decrease in k_1 was observed following exposure to the low PMB concentration, in contrast to the slight increase observed following exposure to the large PMB concentration (Fig. 3). These differences in the viscoelastic parameters for high and low PMB concentrations are likely due to the depolarization of the cytoplasmic membrane that occurs for concentrations greater than 20 μg/mL[45,46] showing that the AFM creep deformation experiment can distinguish between this difference in mechanism of action.

References:

[S1] K. K. H. Poon, E. L. Westman, E. Vinogradov, S. Jin, and J. S. Lam, *J. Bacteriol.*, 2008, **190**, 1857–1865.

Table S1: Best-fit average values of the viscoelastic parameters obtained by fitting the histograms shown in Figs. 3 and 4 to Gaussian distributions. The quoted uncertainties are the half widths at half maxima of the best-fit Gaussian distributions.

	k_1 (N/m)	k_2 (N/m)	η_2 (Ns/m)	$1/\eta_1$ (m/Ns)	τ (s)
Before PMB[1] ($N = 114$)	0.154 ± 0.024	0.86 ± 0.25	0.42 ± 0.11	0.006 ± 0.021	0.42 ± 0.08
After PMB[1] ($N = 135$)	0.174 ± 0.039	0.24 ± 0.08	0.13 ± 0.04	0.56 ± 0.13	0.49 ± 0.06
Before PMBN[2] ($N = 83$)	0.145 ± 0.012	0.87 ± 0.23	0.55 ± 0.22	0.011 ± 0.030	0.49 ± 0.21
After PMBN[2] ($N = 121$)	0.130 ± 0.027	0.19 ± 0.06	0.12 ± 0.03	0.34 ± 0.11	0.58 ± 0.11

[1] data shown in Fig. 3; [2] data shown in Fig. 4

Supplementary Movie S1:

Movie corresponding to a time series of optical microscopy images of *P. aeruginosa* PAO1 bacterial cells following the introduction of 50 μg/ml PMB. The time between images is 1 min. No growth or motion was observed for almost all of the cells, indicating that the cells were not viable after the PMB treatment.

Supplementary Movie S2:

Movie corresponding to a time series of optical microscopy images of *P. aeruginosa* PAO1 bacterial cells following the introduction of 50 μg/ml PMBN. The time between images is 1 min. The cells were observed to move, grow and divide during the 1 h period after PMBN was introduced, indicating that there was no measurable change in the viability of the cells.

Figures
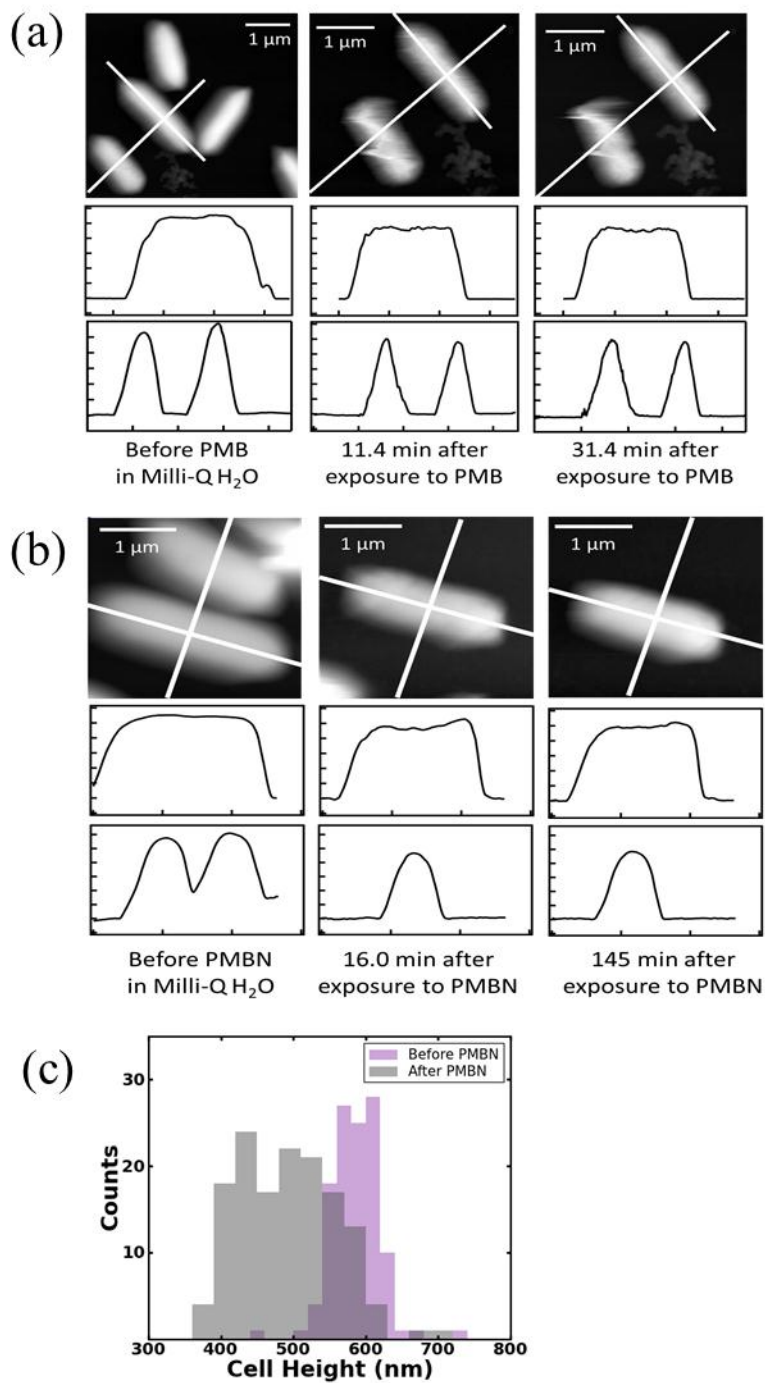
Figure S1: AFM topography images and line scans of *P. aeruginosa* PAO1 bacterial cells before and after exposure to (a) 50 μg/mL PMB, and (b) 50 μg/mL PMBN. The

distance between tick marks corresponds to 100 nm on the vertical axis, and 1.0 µm on the horizontal axis, respectively, for line profiles in both (a) and (b). (c) Histograms of cell heights h before (light purple, $h = 580 \pm 20$ nm) and more than 1 h after (grey, $h = 470 \pm 50$ nm) treatment of 50 µg/mL PMBN. The overlap between the two histograms is indicated by the darker colour.
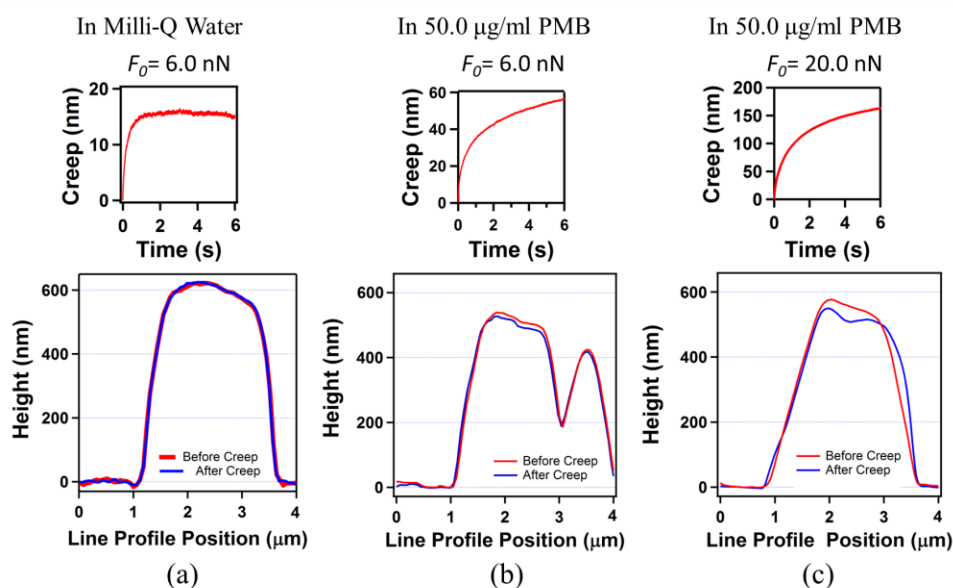
Figure S2: (a) AFM line profiles across a bacterium in Milli-Q water before and after a creep measurement was performed at $F_0 = 6.0$ nN for 6.0 s, showing no significant difference in cell height. The line scans were obtained from AFM topography images collected using a 600 nm dia SiO_2 colloidal tip in contact mode with an applied force of 1 nN. The corresponding creep deformation curve is also shown. (b) AFM line profiles across the same bacterium as in (a), before and after a creep measurement was performed at $F_0 = 6.0$ nN for 6.0 s after 1.5 h of exposure to 50 µg/mL PMB, showing an irreversible decrease in cell height of 15 nm. The line scans were obtained from AFM topography images collected using a 600 nm dia SiO_2 colloidal tip in contact mode with an applied force of 1 nN. The corresponding creep deformation curve is also shown. (c) AFM line profiles across a different bacterial cell before and after a creep deformation experiment was performed at $F_0 = 20.0$ nN for 6.0 s after 2.2 h of exposure to 50 µg/mL PMB, showing an irreversible decrease in cell height of 45 nm. The line scans were obtained from AFM topography images collected using a 600 nm dia SiO_2 colloidal tip in contact mode with an applied force of 1 nN. The corresponding creep deformation curve is also shown.
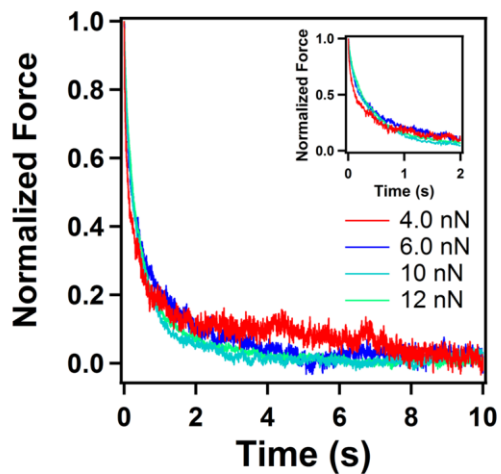
Figure S3: Applied force divided by the set point force F_0 (normalized force) versus time for force-relaxation experiments performed on the same *P. aeruginosa* PAO1 cell for different values of F_0. The inset is an expanded view of the behavior measured for early times ($t < 2$ s).
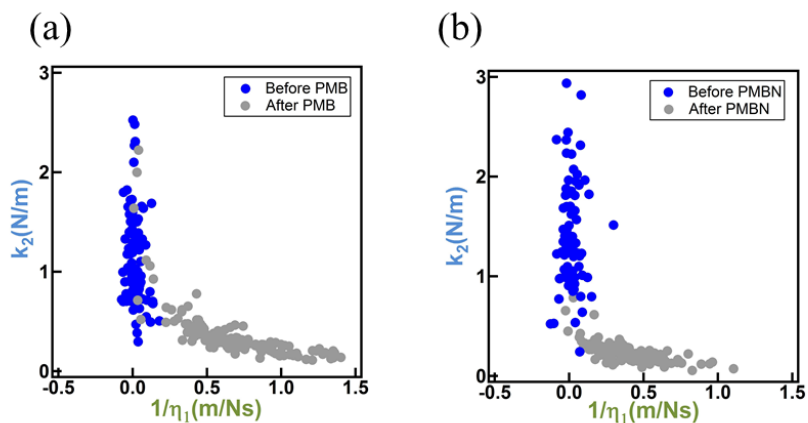
Figure S4: Best fit values of k_2 versus $1/\eta_1$ for *P. aeruginosa* PAO1 bacterial cells before and after exposure to (a) 50 µg/mL PMB (same cells in Fig. 3) and (b) 50 µg/mL PMBN (same cells in Fig. 4). A negative correlation between k_2 and $1/\eta_1$ is observed in both cases after exposure to the peptides.
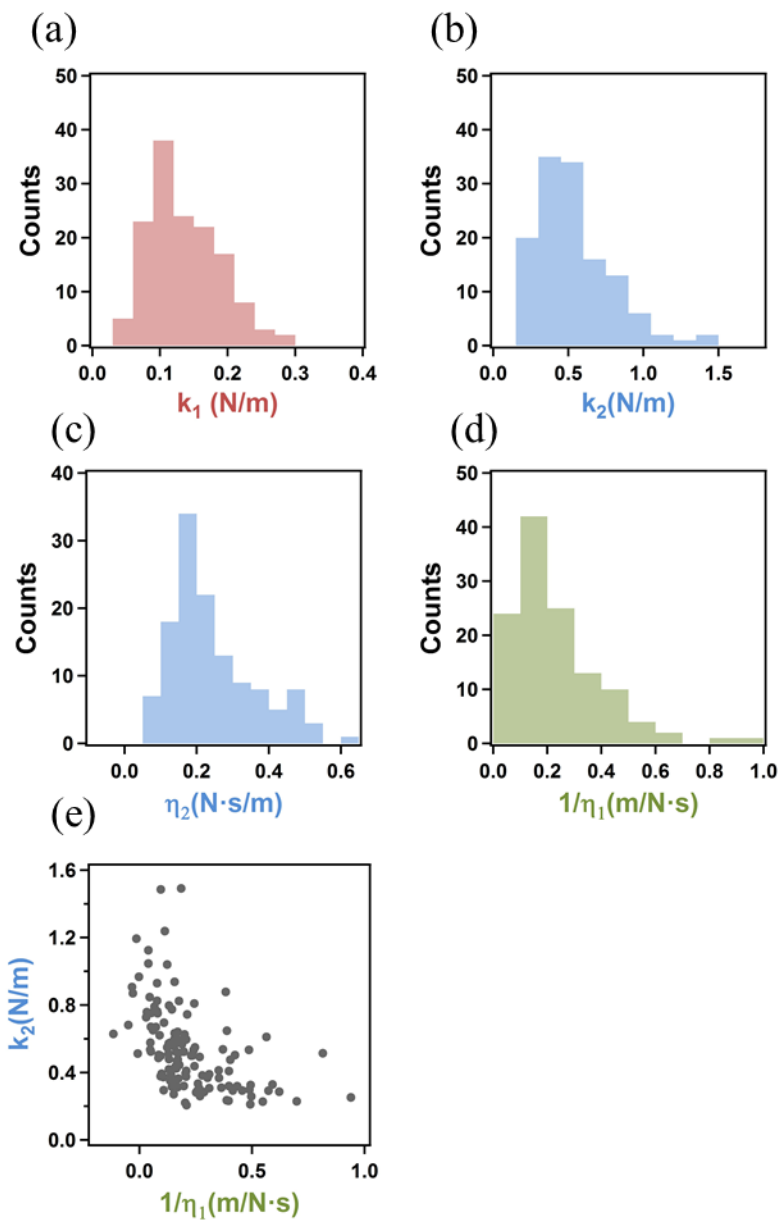
Figure S5: (a)-(d) Histograms of viscoelastic parameters of k_1, k_2, η_2, and $1/\eta_1$ of *P. aeruginosa* PAO1 LPS O-antigen *wapR* mutant cells in Milli-Q water; and (e) plot of k_2 versus $1/\eta_1$, which shows a negative correlation between the delayed elasticity k_2 and permeability $1/\eta_1$ parameters. The viscoelastic parameters are defined in the schematic diagrams shown in Fig. 2.
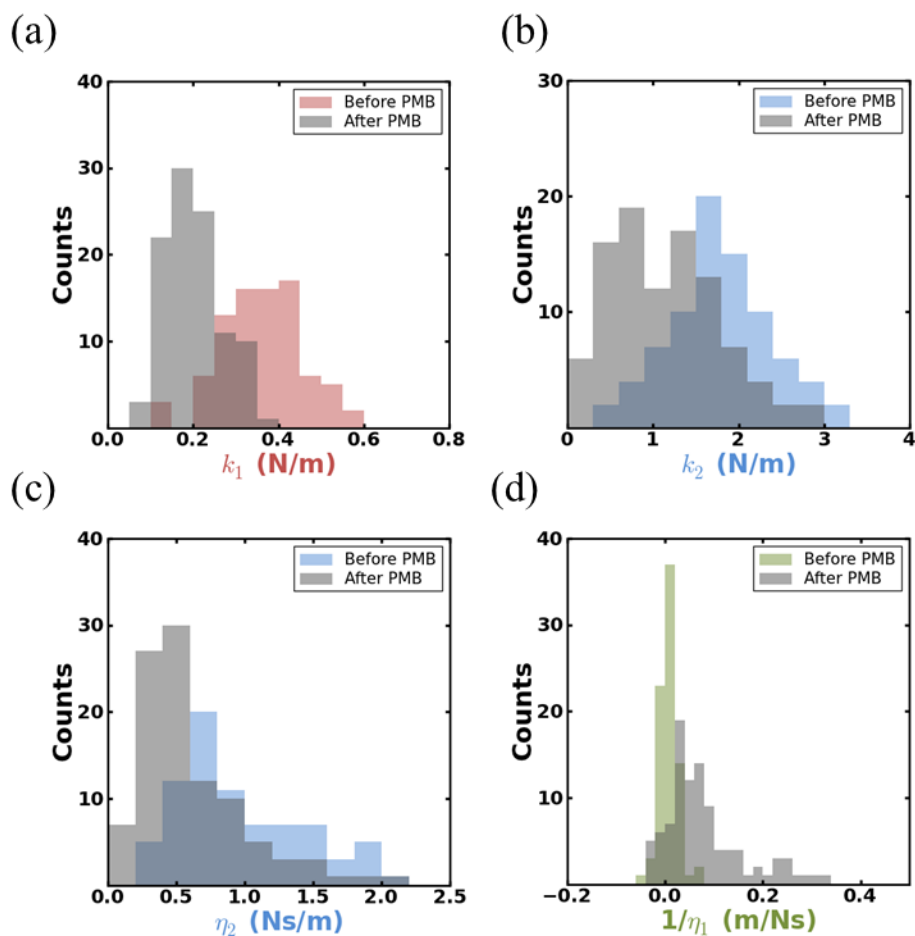
Figure S6: Histograms of viscoelastic parameters (a) k_1, (b) k_2, (c) η_2, and (d) $1/\eta_1$ for *P. aeruginosa* PAO1 cells before and more than 1 hour after being treated with a lower concentration of 5 μg/mL of PMB, measured using cantilevers with 1 μm dia colloidal tip and a spring constant of 0.06 N/m. The viscoelastic parameters are defined in the schematic diagrams shown in Fig. 2. For each plot, the overlap between the two histograms is indicated by the darker colour.